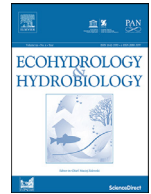




Contents lists available at ScienceDirect

Ecohydrology & Hydrobiology

journal homepage: www.elsevier.com/locate/ecohyd

Original Research Article

Climate change impact on water balance and hydrological extremes in different physiographic regions of the West Seti River Basin, Nepal

Aakanchya Budhathoki^{a,*}, Mukand S. Babel^a, Sangam Shrestha^a, Gunter Meon^b, Ambili G. Kamalamma^a^a Water Engineering and Management, Asian Institute of Technology, Pathumthani 12120, Thailand^b Department of Hydrology, Technische Universität Braunschweig, D-38106 Braunschweig; Germany

ARTICLE INFO

Article history:

Received 8 April 2020

Revised 4 July 2020

Accepted 8 July 2020

Available online xxx

ABSTRACT

This study aims to evaluate the impacts of climate change on water balance components, mainly precipitation, water yield, and evapotranspiration and hydrological extremes in three physiographic regions namely the Middle Mountain region, the High Mountain region, and the High Himalayas region of the West Seti River Basin (WSRB) in Nepal. The future climate was projected using the climate data of three Regional Climate Models (RCMs). The projected future climate data was then fed into the hydrological model, Soil and Water Assessment Tool (SWAT), to simulate hydrologic responses including water balance components under future climate conditions. Results showed that the Middle Mountain region of the basin is expected to receive the highest increase of in precipitation (11.2%) and in water yield (18.2%) as compared to the other two physiographic regions. Conversely, the High Himalayas are expected to have the highest increase of evapotranspiration (19.9%) as compared to the Middle Mountain and High Mountain regions. Similarly, the low flows in the basin are expected to decrease by -15.5% and -19.3% under Representative Concentration Pathway (RCP) 4.5 and 8.5 scenarios, respectively. Whereas high flows are expected to increase by 10.7% under both the RCP scenarios. The results of this study will be helpful to planners and decision makers to formulate adaptation strategies in water resources development and planning such as irrigation and hydropower development.

© 2020 European Regional Centre for Ecohydrology of the Polish Academy of Sciences.

Published by Elsevier B.V. All rights reserved.

1. Introduction

Nepalese River Basins are highly vulnerable to climate change. The West Seti River Basin (WSRB) drained by the Seti River is one of the most vulnerable basins with regard to the probable effects of climate change (Gurung et al., 2015). Several studies reported that the basin is highly

sensitive with the coping capacity of the community to react with climate-induced hazards such as floods, landslides, droughts (Siddiqui et al., 2012). Due to the varied physiography and topography of the WSRB, the water resources planners face difficulties and with the likely climate change, deglaciation in the Himalayan region will have a prominent consequence in the basin. Both physical and climatic factors that affect the vulnerability are to be considered for water resources planning and development. Therefore, evaluation of the impact of climate change in

* Corresponding author: Aakanchya Budhathoki.

E-mail addresses: aakanchya.bc@gmail.com, aakanchya@ait.ac.th (A. Budhathoki).<https://doi.org/10.1016/j.ecohyd.2020.07.001>

1642-3593/© 2020 European Regional Centre for Ecohydrology of the Polish Academy of Sciences. Published by Elsevier B.V. All rights reserved.

different physiographic regions is necessary for water resources planning, development, and management.

Anthropogenically induced climate change is manifested globally in the past as changes in temperature and precipitation patterns and in sea levels rise. These have an impact on hydrological processes, which in turn affect all aspects of water management. The close relationship that exists between water management and socio-economic development proves that achieving sustainable development goals for water, food production, and poverty alleviation is a major challenge with respect to climate change. The 5th Assessment Report (AR5) by the Intergovernmental Panel on Climate Change (IPCC) reported that global ocean and land temperatures have increased by 0.85 °C over the period of 1880 – 2012 (IPCC, 2014). The global average temperature increase is projected to be between 0.3 °C to 4.8 °C by the end of the century (Stocker, 2014). The quality, availability, and supply of water may be affected due to the impact of climate change in water resources (Middelkoop et al., 2001).

There is a significant variation in the spatial and temporal distribution of water on the earth's surface, which will further be aggravated due to the impacts of climate change. Studies reported the potential fluctuations in precipitation among wet and dry areas and seasons (Stocker, 2014) and Himalayan basins are particularly sensitive to the changing climate; a rise in streamflow in the future is projected due to changes in precipitation and glaciers melting (Immerzeel et al., 2013). Water availability is projected to increase in the 21st century in Himalayan basins as the streamflow here is dominated by snow and glacier melt (Lutz et al., 2014). The consequences of increased flows will be experienced as an increase in the frequency of hydro-meteorological extremes, leading to more frequent and more intense natural disasters. Hence, it is very important to understand the seasonal patterns of precipitation and temperature in mountainous regions and the impacts that they have may on water resources (Ficklin et al., 2009).

Several studies reported that climate variability and its frequency are reflected by climate models such as General Circulation Models (GCMs) and Regional Climate Models (RCMs). The understanding of future climate changes is depicted by these GCMs and RCMs with the help of physical components of the atmospheric climate system (Gosling and Arnell, 2016). Since GCMs have a coarser resolution, RCMs have been widely used due to its high spatial resolution for the depiction of future temperature and precipitation in a basin (Anjum et al., 2019). Representative Concentration Pathways (RCPs) scenarios that estimate the radiative forcing (RF) that are based on the multi-model ensembles of Coupled Model Intercomparison Phase Five (CMIP5) (Taylor et al., 2012). These RCPs are the major source of high-resolution climate variation and change studies and different RCP consists of various presumption of population, economy, land use and energy use (Tapiador et al. 2019). The climate scenarios projected by climate models are often fed into hydrologic models for studying the impact of climate change on water resources. These hydrologic models simulate the hydrologic processes in a watershed.

The geophysical and socio-economic conditions of Nepal make it more susceptible to climate change (Aryal and Rajkarnikar, 2011), with considerable temporal and seasonal variations in key climatic parameters. Nepal has a diverse climate condition that ranges from the tropical climate in the south to alpine climate in its northern regions (Shrestha and Aryal, 2011). These changes can alter the responses of hydrologic systems, leading to glacier retreats, the disappearance of natural springs, loss of or operative changes in wetlands, and increased divergence in streamflow. These impacts will undermine the livelihoods of the people of Nepal, particularly the poor (Aryal and Rajkarnikar, 2011). The impacts are also expected to be higher at smaller spatial and temporal scales (Bharati et al., 2014). Studies reveal a rise up to 5.8 °C on the average surface temperature in Nepal towards the end of this century (Bartlett et al., 2010). The fluctuations in temperature and precipitation patterns directly alter the hydrological regime of the basins. The projected annual increases in flow indicate that parts of Nepal, such as the Bagmati River Basin, may become wetter in the future (Babel et al., 2014). The ensemble of GCMs results predict the increase in future streamflow in Bheri River Basin, which is located in the far-western region of Nepal, The expected increase is between 6.2 to 7.3% and 6.0 to 12.5% in RCP 4.5 and RCP 8.5 respectively (Mishra et al., 2018). In the Kaligandagi River Basin of Nepal, the water yield would increase up to 41 to 51% and evapotranspiration will increase 7 to 14% under different scenarios by the end of the century (Bajracharya et al., 2018).

The Government of Nepal is planning to build a hydropower project with a capacity of 750 MW in the WSRB to solve the electricity cutoffs during peak demand as well as to bring economic benefit to the country. Extreme variability in precipitation due to change in climate will have an adverse effect on such development projects by increasing the risk from flash floods, sedimentation, and large boulders. Also, as most of the hydroelectric plants are run-of-the-river type, which could be threatened due to prolonged drought situations. Climate-induced drought conditions could also affect the ecological flow in the lower physiographic region.

To fill this knowledge gap, this study projected future climate scenarios and their impacts on water balance components in the different physiographic regions in the study basin. Furthermore, this study also analyzed the changes in high and low flows due to the changing climate which will affect the water resources development projects in the basin. Three selected RCMs and two future RCP scenarios for each RCMs were used in the study for a baseline of 1986 to 2005 and two future time periods: Near Future (NF) from 2021 to 2040 and Mid Future (MF) from 2041 to 2060.

2. Materials and methods

2.1. Study area

The WSRB (Fig. 1) extends from latitude 30°04' N to 28°56' N and longitude 80°36' E to 81°36' E and has a catchment area of 7,427 km². Facing south with the slant

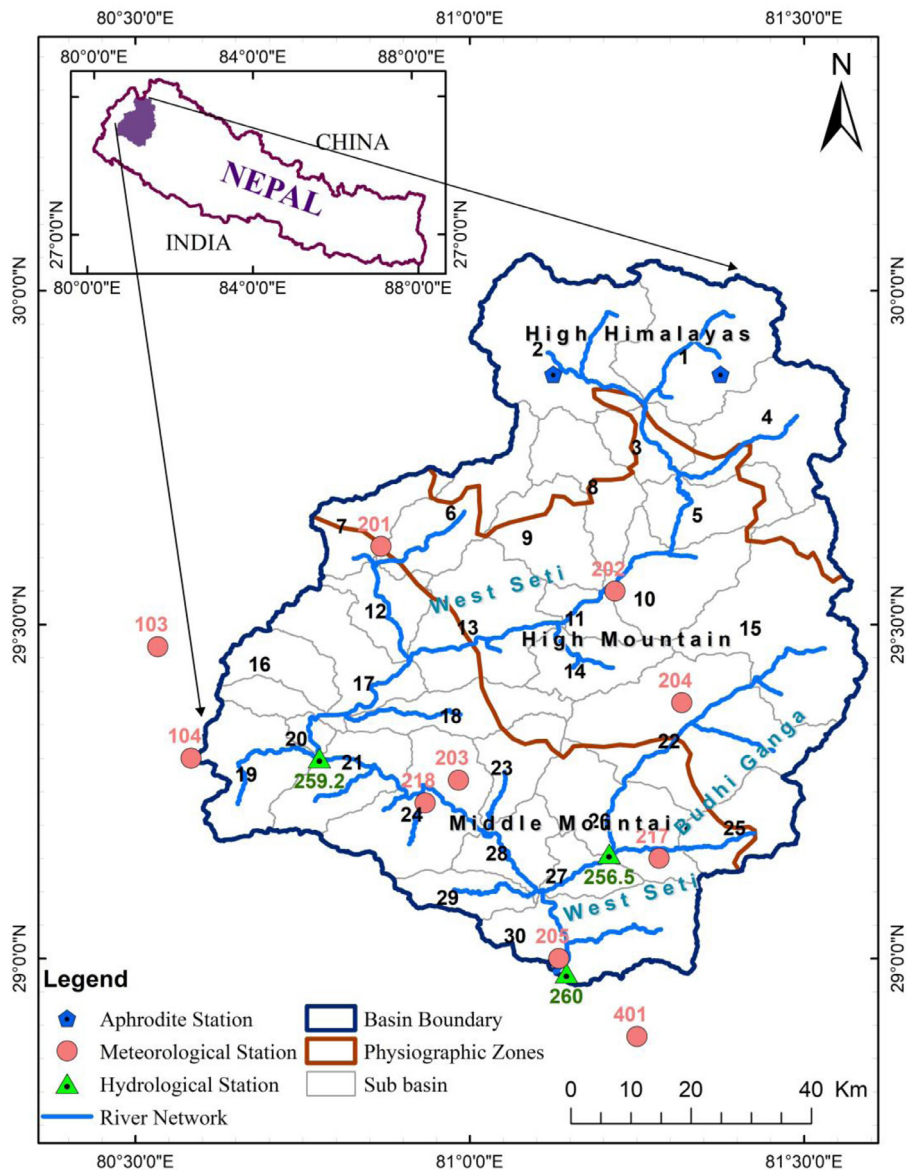


Fig. 1. Location map of WSRB in Nepal and hydro-met stations used in the study.

of the Himalayas, the river in this basin emerges from the glaciers and snowfields around the peaks of Api and Nampa. The elevation varies from 335 meters above sea level (m.a.s.l.) at the basin outlet to 7043 m.a.s.l. at the high mountain range that includes the peaks of Api and Nampa. The average elevation of the basin is approximately 2505 m.a.s.l. Based on the geology, elevation, climate, agriculture, industry, and people, Nepal is categorized into five physiographic regions: Terai, the Siwalik Hills, the Middle Mountain region, the High Mountain region, and the High Himalayas. These regions cover 14%, 13%, 30%, 20%, and 23% of the total area respectively (Matthews, 2001). The elevation ranges of the physiographic regions are: Terai (100 to 200 m.a.s.l.), Siwalik (700 to 1,500 m.a.s.l.), Middle Mountain (1,500 to 2,700 m.a.s.l.), High Mountain (2,000 to 4,000 m.a.s.l.), and High Himalayas are (4,000

to 8,848 m.a.s.l.) (Shrestha and Aryal, 2011). The southernmost Terai region is the most fertile area where intensive agriculture is practiced. The Siwalik region is rough and uneven and is often adversely affected by natural disasters such as floods and landslides. The Middle Mountain region supports a large human population and although most of the area is rugged topography, agriculture occupies a substantial part of the region. The High Mountain region lies under the snow line followed by the northernmost High Himalayan region which extends up to the highest summit in the world (Matthews, 2001). Although Nepal is classified as a subtropical region, due to its distinctive geographical as well as topographical distributions within a short extent of 140 km north to south, it has vast climatic and environmental diversity (Shrestha and Aryal, 2011).

In accordance with the physiographic regions mentioned above, the WSRB covers three physiographic regions: the Middle Mountain regions, the High Mountain region, and the High Himalayas. Each region respectively covers an area of 3001 km², 2734 km², and 1692 km² in the basin. There are ten meteorological stations present in the study area and out of them three lies in the High Mountain region and the remaining seven in the Middle Mountain region. Since the High Himalayas region do not have any monitoring station, APHRODITE data were used as mentioned in [section 2.2](#). In addition, all three hydrological stations in the basin lie in the Middle Mountain region. The average annual rainfall in the basin is 1980 mm (1986 to 2005). Rainfall during winter (December to February), pre-monsoon (March to May), monsoon (June to September), and post-monsoon (October and November) seasons is 142 mm, 262 mm, 1518 mm, and 57 mm respectively. More than 75% of the annual rainfall in this basin is received during the monsoon season. The average annual temperature in the basin is 19 °C, with an average minimum of 12.1 °C and an average maximum of 25.8 °C. The annual average discharge of the West Seti River is 296.2 m³/s.

2.2. Data

2.2.1. Topographic, soil, and land use data

The Digital Elevation Model (DEM) in this research was acquired from the Advanced Spaceborne Thermal Emission and Reflection Radiometer (ASTER) Global Digital Elevation Model Version 2 (GDEM V2) with a 1-arc second (approximately 30 m at the equator) resolution (<http://reverb.echo.nasa.gov/reverb>). A major part of the area of the basin has an elevation between 2000 and 6000 m.a.s.l. as shown in Supplementary Fig. S1. The maximum elevation is 7043 m.a.s.l. and minimum elevation is 335 m.a.s.l. in the basin.

The soil map of the year 1986 was acquired from the National Land Use Project (NLUP) in association with the Ministry of Land Reform and Management (MoLRM), Nepal at scale 1: 50,000. A total of 23 soil types are available in the basin. The dominant soil types in the Middle Mountain region of the basin are eutric cambisols and chromic cambisols whereas the dominant soil type in the High Mountain region is dystric regosols and in the High Himalayas are rocky outcrop and snow cover. The land use map of 300 m resolution for the year 2010 was obtained from the European Space Agency (<http://due.esrin.esa.int/globcover/>). Ten different land use types are observed in the basin area, with the maximum area occupied by deciduous and evergreen forests, followed by agricultural land. The Middle Mountain and the High Mountain regions are predominantly covered by agricultural land and forests whereas the High Himalayas region is mostly covered with snow and hay. The DEM, soil, and land use map are presented as in Supplementary Fig. S2, S3 and S4, respectively.

2.2.2. Observed historical meteorological and hydrological data

Daily data of minimum and maximum temperature and precipitation from 1980 to 2014 were gathered from the Department of Hydrology and Meteorology

(DHM), Nepal. The upper area of the basin where the station data is not available, Asian Precipitation – High Resolved Observational Data Integration (APHRODITE); (<https://climatedataguide.ucar.edu/climate-data/aphrodite-asian-precipitation-highly-resolved-observational-data-integration-towards>.) data was used for the base period. APHRODITE's project on Water Resources has been conducted since 2006 with a grid size of 0.25° above the Monsoon Asia region (Yatagai et al., 2012). It is found that the APHRODITE dataset could be incorporated in the High Himalayan region along with available temperature and precipitation station data. Depending on the data availability and placement, ten meteorological stations were used in the study from DHM, and the APHRODITE data was used at two locations ([Fig. 1](#)). These data have not been corrected to any wind effect. In addition, the homogeneity test of the observed data was conducted based on cumulative deviations from the mean as suggested by [Buishand, 1982](#). Data from the meteorological stations were spatially interpolated using the Thiessen polygon technique and input to the hydrologic model to produce a gridded map of climate input. The higher elevation region of the basin is mountainous, with peaks and valleys; hence, the interpolated meteorological data was not able to exactly represent the variability of the mountainous region. Therefore, lapse rates of temperature and precipitation were taken within each sub-basin to extrapolate temperature and distribute precipitation based on the different elevations. In each band, the temperature and precipitation were calculated as a function of lapse rate and the gage and the average elevation variation was specified for each band ([Neitsch et al., 2011](#)).

Based on the availability of temperature stations, an average temperature lapse rate of -5.3 °C/km was calculated. Similarly, depending on the available precipitation stations, the average precipitation lapse rate of 200 mm/km was calculated. [Table 1](#) presents the meteorological stations and data available for each specific station with the hydrological stations in and near the study basin. The correlation plot between observed station data and APHRODITE data is illustrated in Supplementary Fig. S5. It is established that there is a consistent bias between the observed data at the stations and data from APHRODITE. The monthly bias correlation factor was determined using the APHRODITE climate data with observed climate data and based on the factor bias correction was applied to the APHRODITE station data that was used in the study.

Three hydrological stations as given in [Table 1](#) were considered for calibration and validation of the hydrologic model. At outlet, the Banga station, the average annual discharge is 296.2 m³/s.

2.2.3. Future climate data

Five RCMs developed by CSIRO Marine and Atmospheric Research, Australia, namely ACCESS-CSIRO-CCAM (ACCESS), GFDL-CM3-CSIRO-CCAM (GFDL), MPI-ESM-LR-CSIRO-CCAM (MPI), NCC-NorESM1-M-CSIRO-CCAM (NorESM), and CNRM-CM5-CSIRO-CCAM (CNRM) from driving GCMs ACCESS1.0, GFDL-CM3, MPI-ESM-LR, CCSM4, NorESM-M, and CNRM-CM5 respectively were initially selected. Statistical parameters of the observation were con-

Table 1

Summary of hydro-met stations and the data applied in the WSRB.

Meteorological stations				
Station Code	Station Name	Latitude (°N)	Longitude (°E)	Variable
103	Patan	29.47	80.53	Rainfall, Tmax, Tmin
104	Dadeldhura	29.30	80.58	
202	Chainpur	29.55	81.22	
203	Silgadhi	29.27	80.98	
401	Pusma Camp	28.88	81.25	
201	Pipalkot	29.62	80.87	Rainfall
204	Bajura	29.38	81.32	
205	Katai	29.00	81.13	
217	Mangalsen	29.15	81.28	
218	Dipayal	29.23	80.93	Tmax, Tmin
Hydrological stations				
Station Code (Name)	Catchment area (km ²)	Latitude (°N)	Longitude (°E)	Average Annual Discharge (m ³ /s)
256.5 (Mangalsen)	1659	29.16	81.21	85.2
259.2 (Gopaghat)	4341	29.30	80.78	199.1
260 (Banga)	7427	28.98	81.14	296.2

sidered to evaluate the performance of the models. Based on the performance statistics namely, the Coefficient of Determination (R^2), Root-Mean-Square Error (RMSE), and Mean Absolute Error (MAE) as presented in Supplementary Table S1, ACCESS, GFDL, and MPI with a grid size of $0.5^{\circ} \times 0.5^{\circ}$ were chosen for future climate data analysis. These RCMs were downloaded from the <http://cccr.tropmet.res.in/home/index.jsp> cordex data website. Daily historical (1970 to 2005) data and future climate data (2006 to 2099) with emission scenarios, RCP 4.5 and RCP 8.5 were used for the analysis. The RCP 4.5 scenario is a stabilization scenario, which means the radiative forcing level stabilizes at 4.5 W/m^2 before 2100 by the employment of a range of technologies and strategies for reducing greenhouse gas emissions. Whereas RCP 8.5 corresponds to the pathway with the highest greenhouse gas emissions leading to a radiative forcing of 8.5 W/m^2 at the end of the century. A total of five grid cells of the selected RCMs covered the study basin.

For the climate change and impact analysis, the climate data of baseline (BL) period of 1985 – 2005 and the future periods classified as Near Future (NF), i.e. 2021 to 2040, and Far Future (FF), i.e. 2041 to 2060 were taken from the outputs of the selected RCMs. Since GFDL had future data available only till 2070, the period of analysis considered for this study was until 2060.

2.3. Methodology

The presented study in WSRB evaluated the future climate and its consequences on three major water balance components considering the physiographic regions. Soil and Water Assessment Tool (SWAT) model was used to simulate the hydrology and water balance components in the basin. Fig. 2 presents the overall methodology adopted for the study.

2.3.1. Future climate projection

For this research, three RCM models of CCAM which are ACCESS, GFDL, and MPI were carefully chosen on the basis of the resolution, vintage, representativeness, and validity (Smith et al., 1998). It is necessary to bias correct the outputs from selected RCMs. Based on the performance statistics R^2 for precipitation, quantile mapping showed preferable results in comparison to linear scaling, while for temperature, linear scaling was found to be better than the quantile mapping. As stated in Section 2.2.3, identified three models were bias corrected using linear scaling and quantile mapping for future climate data. RCM simulated temperature data bias were removed using linear scaling (Fang et al., 2015) and precipitation data bias were removed using quantile mapping (Maraun, 2013).

2.3.2. Hydrological modeling

Hydrological assessment in the study was conducted by applying a hydrological model, Soil and Water Assessment Tool (SWAT) which is a semi-distributed physical-based model widely used to simulate hydrology and obtain water balance components to analysis different management scenarios (Neitsch et al., 2011). It distributes a watershed into multiple sub-watersheds or sub-basins for simulation. These are additionally apportioned into hydrological response units (HRUs) which are a coalition of land use, soil type, and management properties (Neitsch et al., 2011). The water balance Eq. (1) is used to simulate the hydrologic cycle.

$$SWC_t = SWC_0 + \sum_{i=1}^n (R_{day} - Q_{surface} - E_a - w_{seep} - Q_{gw}) \quad (1)$$

Where,

t = Time (day)

SWC_t = mm of final water content in soil.

SWC_0 = mm of initial water content in soil

R_{day} = mm of precipitation for i th day.

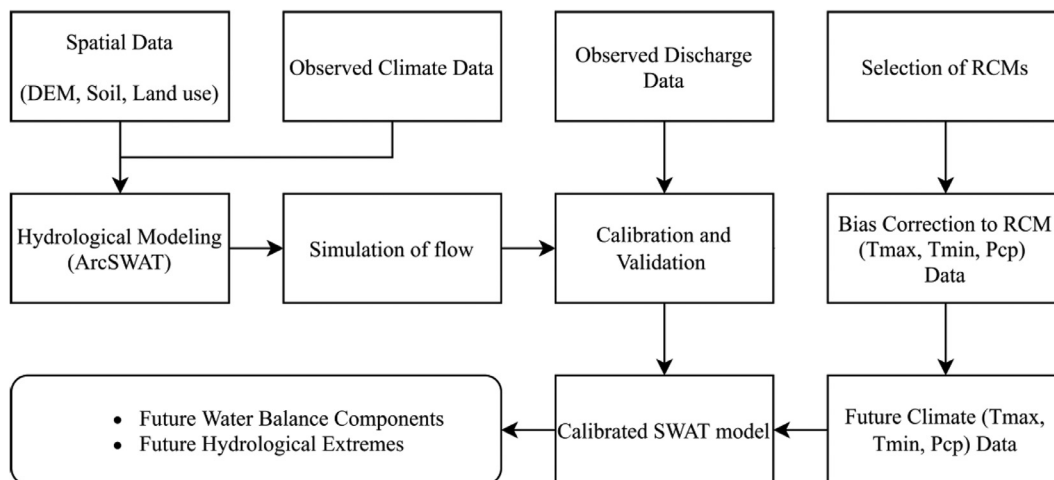


Fig. 2. Flowchart of methodology adopted in this study.

$Q_{surface}$ = mm of surface runoff for i th day.

E_a = mm of evapotranspiration for i th day.

w_{seep} = mm of percolation for i th day.

Q_{gw} = mm of return flow for i th day.

The potential evapotranspiration was estimated using the Penman-Monteith method (Neitsch et al., 2011). The HRUs were defined by specifying threshold values of slope, soil, and land use. Thresholds used for land use, soil, and the slope were respectively 0%, 15%, and 10% in the sub-basin. A total of 598 HRUs were defined through this process. Ten elevation bands were selected within the sub-basin to allow disparity in temperature and precipitation with respect to altitude over the basin (Grusson et al., 2015).

The hydrological model's performance was evaluated by the calibration and validation results. The performance statistics of Nash-Sutcliffe Efficiency (NSE), Coefficient of Determination (R^2), and Percentage Bias (PBIAS) were used. The observed streamflow data from three gauging stations were used for the calibration and validation of the hydrological model for daily and monthly flows. For stations Gopaghat and Banga, the period of 1986 to 1990 was used for calibration and 1991 to 1995 for validation. A 5-year period from 1981 to 1985 was used as the warm-up period, for the model to reach an optimal state. Observed streamflow for the period from 2000 to 2003 (for calibration) and 2004 to 2005 (for validation), with a warm-up period of 1995 to 1999 was used for Mangalsen due to lack of availability of data. The warm-up period helps in stabilizing the initial conditions for groundwater and soil water storage (Fontaine et al., 2002). In this study, a manual calibration based on a trial and error approach was used. It focused on model parameters that were considered most sensitive, as reported by Gurung, et al. (2015).

2.3.3. Analysis of water balance components

Water balance in the SWAT model plays a very crucial role and consists of all the processes happening within the basin (Neitsch et al., 2011). The principal water balance components are precipitation, water yield, and evapotranspiration (Ayivi and Jha, 2018). Eq. (2) and Eq. (3) shows

the relation of water yield and baseflow.

$$\text{Water Yield} = \text{Surface Runoff} + \text{Lateral Flow} + \text{Baseflow} - \text{Transmission loss} \quad (2)$$

$$\text{Baseflow} = \text{Groundwater (Shallow aquifer) flow} + \text{Groundwater (Deep Aquifer) flow} \quad (3)$$

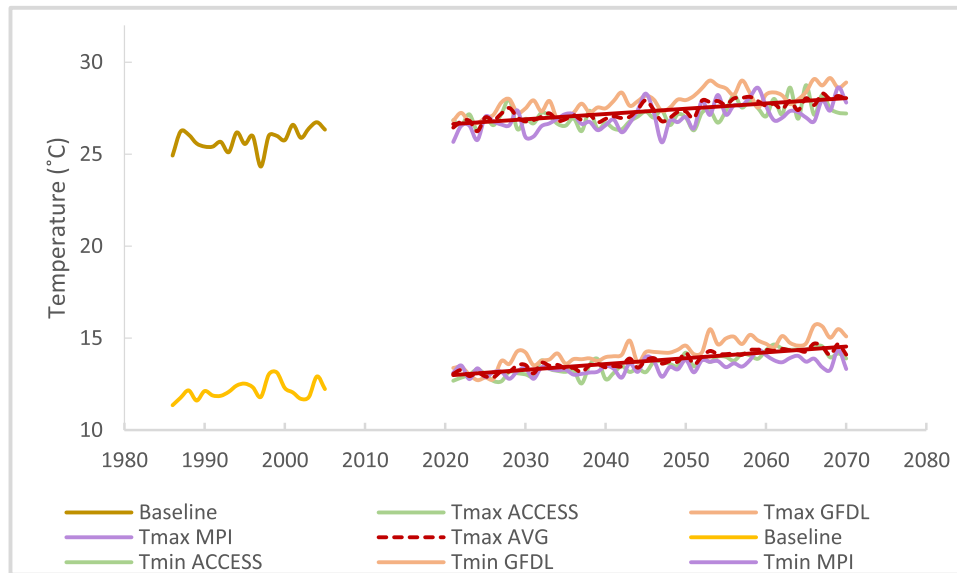
3. Results and discussion

3.1. Future climate scenarios

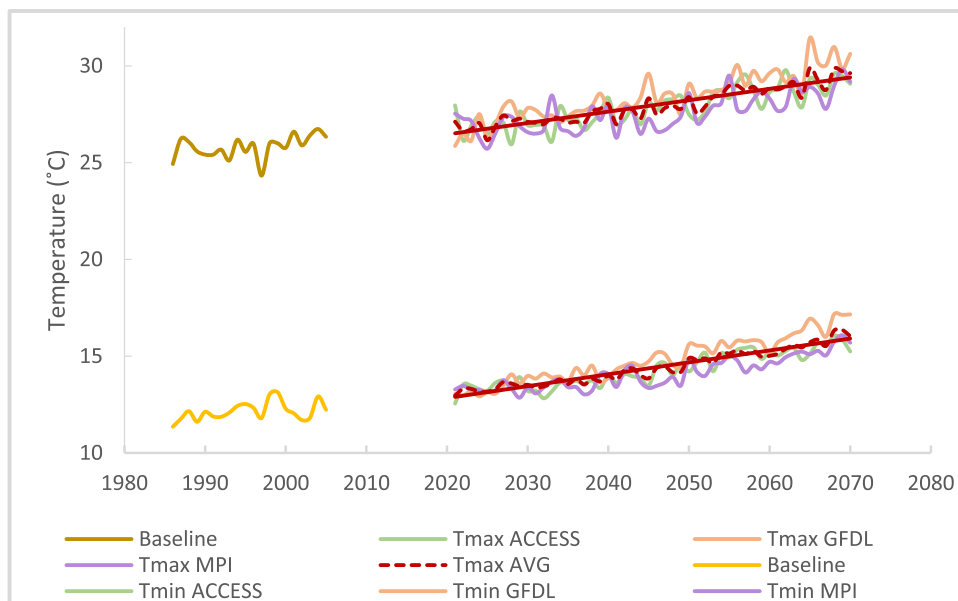
The performance of bias correction for Chainpur station is illustrated in Supplementary Table S2. The bias corrected temperatures show a very good correlation with the observed temperatures. Both minimum and maximum temperatures data, observed and corrected, matched quite well. For minimum temperature, biases are higher in the winter months, whereas for maximum temperature, biases are higher in the summer months (Supplementary Fig. S6).

The quantile mapping method was used for the bias correction of rainfall data. Bias correction of RCM simulated rainfall data shows correction in the mean as well as an improvement in the RMSE, MAE, and R^2 values. This confirmed the validation of this method. The MPI model is more reliable than the other two in simulating precipitation. For ACCESS and GFDL, the biases are higher during the monsoon period (Supplementary Fig. S7).

Fig. 3 (a) and (b) shows the annual average maximum and minimum temperatures of the selected RCMs for RCP 4.5 and RCP 8.5, respectively, and their ensembles, which is the weighted average giving equal weights to all RCMs. An increase in both temperatures is projected in the future for both RCP 4.5 and RCP 8.5. The increase is higher under RCP 8.5 compared to RCP 4.5. The average rise in maximum temperature lies between 0.5 to 3.2 °C under RCP 4.5 and 0.5 to 4.7 °C under RCP 8.5. In the case of precipitation also, an increase in the future is projected under both RCP 4.5 and RCP 8.5 (Fig. 4 (a) and (b)), and a large inter-annual variability is seen in projected precipitation. The average



(a)



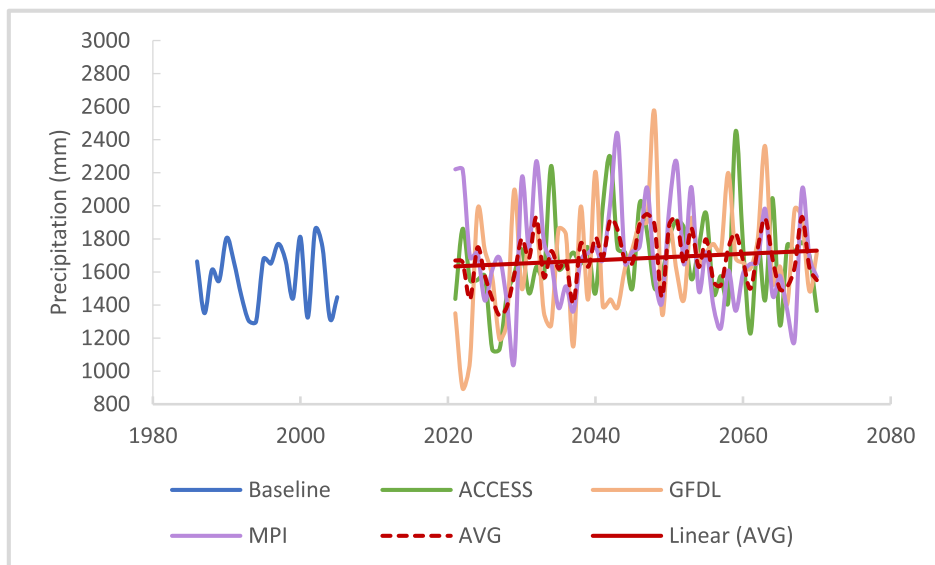
(b)

Fig. 3. Baseline and projected annual maximum and minimum temperature in the WSRB (a) RCP 4.5 (b) RCP 8.5 (Ensemble and individual RCM).

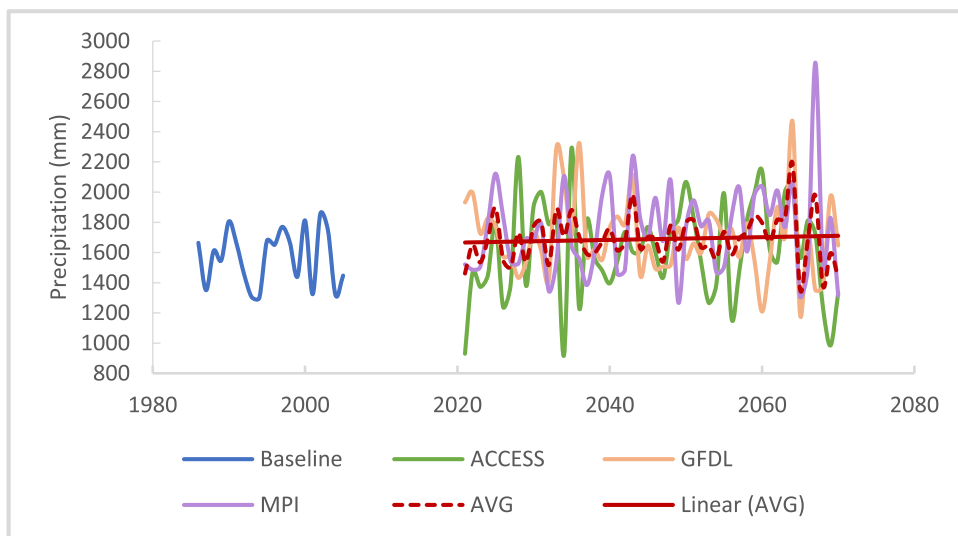
annual precipitation is projected to increase by 6.2% under RCP 4.5 and 7% under RCP 8.5.

Projected seasonal changes in maximum temperature, minimum temperature, and precipitation are described in Supplementary Table S3, S4, and S5 respectively. All the RCMs project both the temperatures to increase in all the seasons. The maximum temperature increase in the summer season (MAM) in the NF is likely to range from 0.4 °C to 2.1 °C under RCP 4.5 and 0.7 °C to 2.8 °C under RCP 8.5. Similar increases, in the range of 0.9 °C to 1.5 °C under RCP

4.5 and 1.2 °C to 2.2 °C under RCP 8.5, are projected for the MF. The minimum temperature in the winter season (Dec-Feb) is expected to increase in the range of 0.7 °C to 1.7 °C under RCP 4.5 and 1.0 °C to 2.3 °C under RCP 8.5 in the NF. The increase in minimum temperature in the MF is in the range of 0.8 °C to 1.3 °C under RCP 4.5 and 1.2 °C to 1.6 °C under RCP 8.5. Projected seasonal precipitation increase is greater in the post-monsoon season (Oct to Nov). Except for MPI, the other two RCMs project an increase in post-monsoon precipitation by up to 54.3% under RCP 4.5.



(a)



(b)

Fig. 4. Baseline and annual average precipitation in the WSRB (a) RCP 4.5 (b) RCP 8.5 (Ensemble and individual RCM).

Under RCP 8.5, other than ACCESS, the two RCMs project similar post-monsoon increases in precipitation up to 47%. For the monsoon season, precipitation increases are projected under both RCP 4.5 and RCP 8.5 by all the RCMs except ACCESS. Monsoon precipitation is projected to increase by 32.8% and 31.1% under RCP 4.5 and RCP 8.5, respectively.

3.2. Performance of hydrological modeling

The calibration and validation outcome for the outlet Banga is presented in Fig. 5. The model simulated hydrological processes in the study basin quite well for

both daily calibration and validation periods, except for some high flows. The model performance for both calibration and validation given in Table 2 indicate that it has performed well (Moriasi et al., 2007) and can be used for simulating hydrologic behavior of the basin under future climate conditions. The discrepancies in the performance statistics, especially in PBIAS could be due to variation in daily observed and over- and under-simulated flows at three hydrological gauging stations with different watershed characteristics and areas used for calibration and validation. As expected, the model's performance is better for monthly flows than for daily flows. This stipulates that long-term flows are better simulated by the model

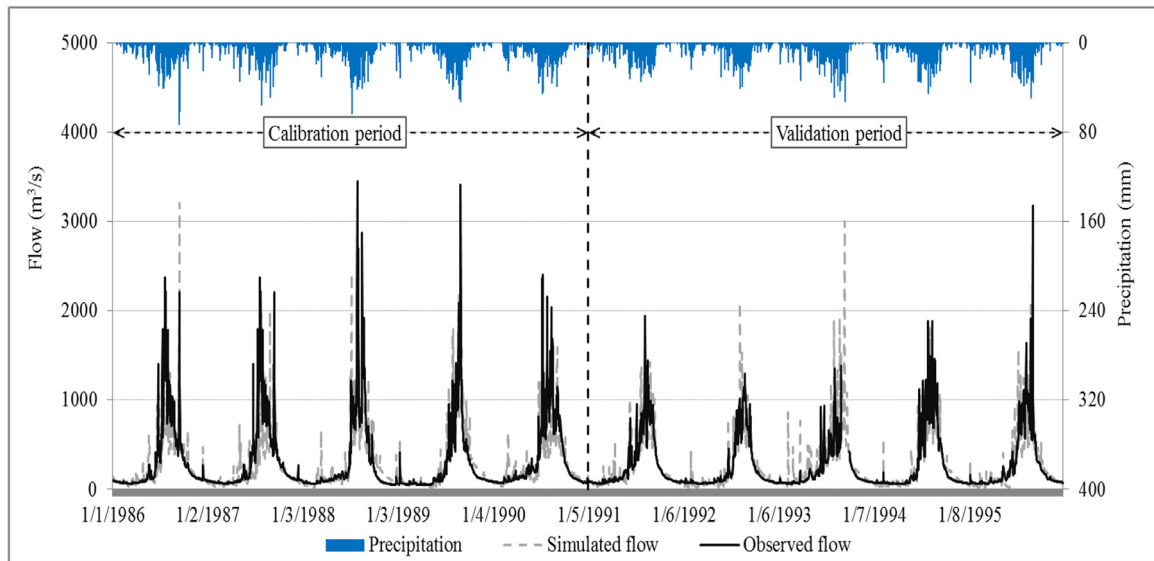


Fig. 5. Observed and simulated daily flow during calibration and validation at the outlet of the WSRB.

Table 2

SWAT model performance during calibration and validation in the WSRB.

Station Code	Period	NSE		R ²		PBIAS
		Daily	Monthly	Daily	Monthly	
259.2	1986 to 1990 (calib.)	0.72	0.86	0.75	0.91	15.9
Seti (Mangalsen)	1991 to 1995 (valid.)	0.62	0.88	0.67	0.95	19.6
256.5	2001 to 2003 (calib.)	0.64	0.82	0.66	0.87	10.9
Budhi Ganga (Gopaghat)	2004 to 2005 (valid.)	0.64	0.95	0.67	0.95	9.2
260	1986 to 1990 (calib.)	0.65	0.83	0.66	0.87	9.2
West Seti (Banga)	1991 to 1995 (valid.)	0.71	0.95	0.72	0.96	0.03

than short-term events. The multi-site calibration results also show that the flows are simulated better at the upstream stations as compared to the downstream ones.

The list of sensitive parameters in the model is shown in Supplementary Table S6. Curve number (CN2) was found as the most sensitive parameter, followed by soil hydraulic conductivity (SOL_K1). The model's results were also sensitive to the precipitation lapse rate (PLAPS), snow fall temperature (SFTMP), snowmelt temperature (SMTMP), and the alpha base flow factor (ALPHA_B).

3.3. Water balance in the WSRB

The model run for the baseline (1986 to 2005) with the calibrated parameters estimated average annual values of the various components of water balance, which are presented in Table 3. The water balance components include precipitation, water yield, and evapotranspiration. The annual average precipitation in the basin is 1979.5 mm and out of it, only 3.5% of the precipitation is contributed by snowfall in the period of baseline. The amount of snow melted and sublimed is more than that which falls. Surface runoff amounts to 15.9% of the average annual precipitation. The average annual evapotranspiration accounts for 36% of the average annual precipitation in the basin.

Table 3

Annual average water balance components of the WSRB during the base period (1986 to 2005) (as simulated by the SWAT model).

Water Balance Component	Amount (mm)
Precipitation	1979.5
Surface runoff (Q)	314.9
Groundwater (Shal AQ) (Q)	420.3
Groundwater (Deep AQ) (Q)	23.4
Water yield	1249.8
Evapotranspiration	711.9

3.4. Impact of climate change on water balance components

3.4.1. Future precipitation

The percentage change in ensemble mean precipitation during different future periods and under different emission scenarios is shown in Fig. 6. An increase in precipitation in the MF is higher than in the NF, with even precipitation increases projected to be more than 15% from the baseline. Considering the different physiographic regions, the Middle Mountain region will experience changes between 2 to 11% in precipitation in both the NF and the MF under both RCP scenarios. Under RCP 4.5 in the MF and RCP 8.5 in the NF, all regions in the basin will experience an increase in precipitation, whereas, in the other two sce-

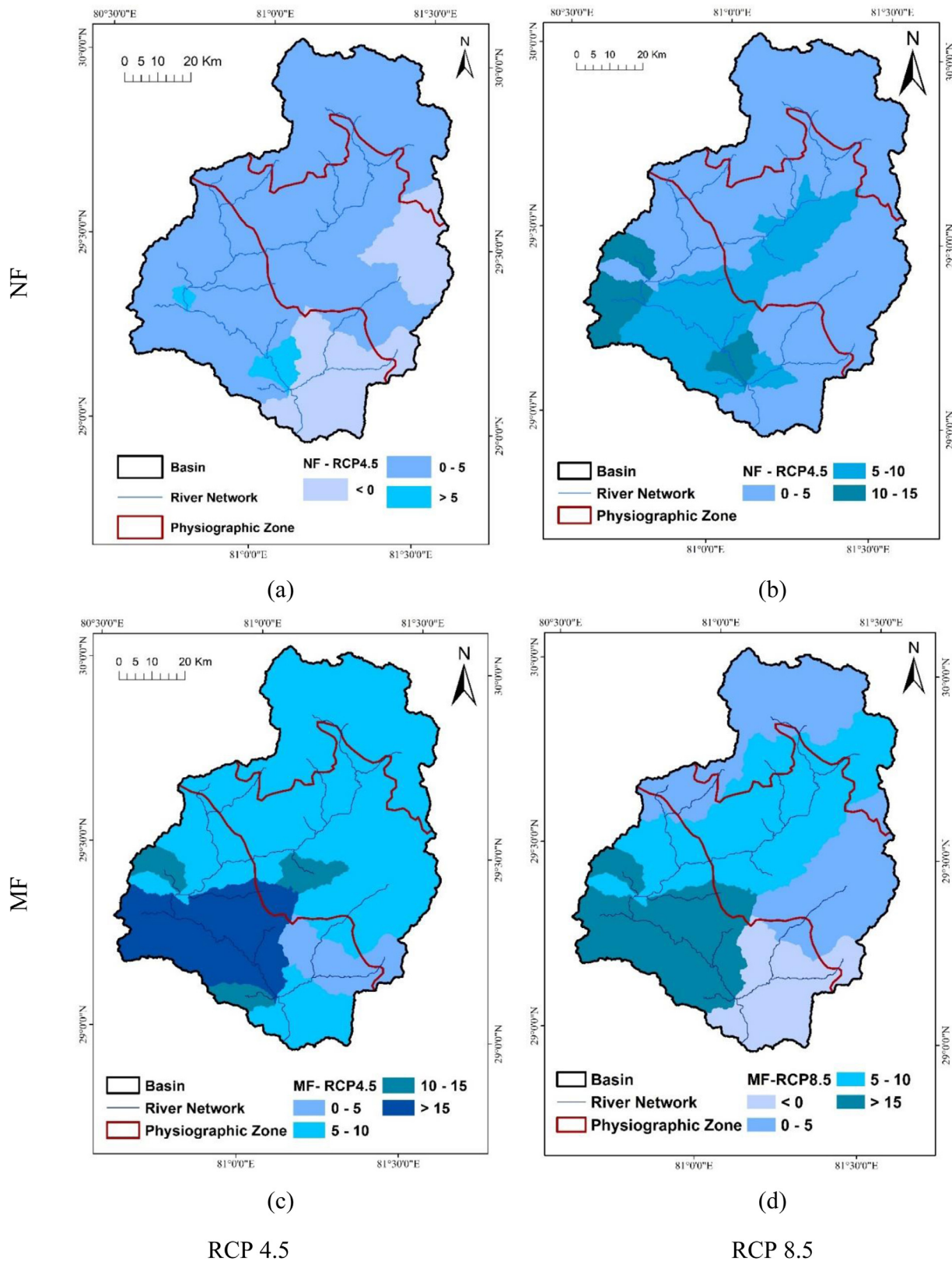


Fig. 6. Percentage change in ensemble mean precipitation under RCP 4.5 and RCP 8.5 scenarios in the NF (a) (b) (Upper Panel) and the MF (Lower Panel) (c) (d) in the WSRB.

Table 4

Percentage changes in water balance components with respect to the baseline in different physiographic regions under RCP 4.5 and RCP 8.5 in the WSRB.

Water Balance Components	Middle Mountain		High Mountain		High Himalayas	
	NF	MF	NF	MF	NF	MF
<i>RCP 4.5</i>						
Precipitation	2.0 (-11.4 to 23.0)	11.2 (3.5 to 21.6)	1.1 (-8.5 to 17.1)	7.8 (-2.0 to 22.5)	1.4 (-6.6 to 7.8)	8.0 (1.0 to 15.3)
Water Yield	3.8 (-29.5 to 57.4)	18.2 (-8.8 to 48.8)	-1.3 (-12.9 to 47.6)	7.6 (5.5 to 48.8)	-1.1 (-11.3 to 10.6)	6.8 (-2.6 to 20.9)
Evapo-transpiration	3.1 (-5.2 to 16.7)	6.7 (-1.5 to 17.0)	6.6 (-3.6 to 24.3)	9.3 (0.1 to 19.8)	13.6 (0.6 to 35.0)	17.2 (6.1 to 34.4)
<i>RCP 8.5</i>						
Precipitation	7.1 (-7.8 to 26.4)	6.9 (-14.4 to 37.9)	4.1 (-6.2 to 20.7)	4.2 (-3.0 to 22.9)	4.0 (-3.5 to 11.6)	5.0 (2.0 to 12.3)
Water Yield	13.1 (-19.5 to 76.3)	10.1 (-30.9 to 87.7)	3.3 (-11.7 to 62.9)	1.0 (-9.3 to 52.7)	1.8 (-7.7 to 16.5)	1.7 (-4.5 to 15.2)
Evapo-transpiration	3.3 (-4.5 to 14.9)	6.2 (-3.5 to 20.6)	6.9 (0.2 to 21.4)	10.9 (0.1 to 20.3)	14.9 (1.6 to 36.7)	19.9 (9.5 to 34.6)

narios, some regions will experience a decrease in precipitation. Similar results are reported by Pandey et al., (2019).

3.4.2. Future water yield

In the High Himalayas and a major part of the high mountains, the water yield is projected to decrease in the NF, and it is projected to increase in all the physiographic regions in the MF under RCP 4.5. However, under RCP 8.5, more areas will experience a decrease in water yield in the MF than in the NF, particularly in the High Mountain region. In the Mid Mountain region, the areas that will experience a decrease in water yield in the NF under RCP 4.5 are projected to have a similar decreasing trend in the MF under RCP 8.5. Under RCP 4.5, in the NF, the majority of the basin area will experience a reduction in water yield whereas, in the MF, the majority of the area in the basin will have a projected increase in water yield in the range of 5 to 10% (Fig. 7). Other studies in Nepal also show that the water yield is expected to increase in the future (Bajracharya et al., 2018).

3.4.3. Future evapotranspiration

The High Himalayan region is expected to have more than a 15% increase in evapotranspiration in the NF, as compared to the baseline values, and this will further increase by more than 20% in the MF (Fig. 8). Similar increases are projected under both RCP 4.5 and RCP 8.5. Most of the High Mountain region is expected to have an increase in evapotranspiration in the range of 10 to 15% in both the NF and the MF under both RCP 4.5 and RCP 8.5. In the Middle Mountain region, a majority of the area will have an ET increase in the range of 0 to 5% in NF and 5 to 10% in the MF. Bajracharya et al., (2018) also reported similar results in the Kaligandaki River Basin in Nepal.

3.4.4. Future water balance in the physiographic regions

Precipitation is expected to increase relatively more in the Middle Mountain region as compared to the other two physiographic regions of the basin (Table 4). Additionally, in the MF, under both RCP 4.5 and RCP 8.5, there is a

greater increase in precipitation as compared to the values in the NF in all the physiographic regions. Following the trend of precipitation, water yield will also increase; the maximum increase will be in the Middle Mountain region, followed by the High Mountain region and then the High Himalayas. Conversely, the percentage change in evapotranspiration in the High Himalayas is more than in the other two physiographic regions. An increase in evapotranspiration in all regions suggests the significant role of warming temperatures in water balance components. The changes in evapotranspiration with elevation might result in some phenological shifts or other vegetation responses. The precipitation increase in the basin is projected to range from -11 to 37% in the different physiographic regions; the High Mountain region will experience a slight increase while the Middle Mountain region a much higher increase.

Alike precipitation, water yield is also expected to increase by about -30 to 62% in the three physiographic regions of the basin. Furthermore, evapotranspiration is projected to increase by about -5.2 to 35% in the three physiographic regions of the basin. These projected changes in precipitation and evapotranspiration follow a gradual increase from the NF to the MF under both RCP scenarios in all the physiographic regions. The findings of this study are in line with the results of Pandey et al., (2019). The net water yield is expected to rise from the NF to the MF under RCP 4.5 whereas, it will decrease from the NF to the MF under RCP 8.5. Similar results are shown in the Koshi Basin of Nepal where the precipitation is likely to increase in the upper part of the basin in the NF and MF whereas, a decrease in the lower part of the basin in NF. Similarly, evapotranspiration is also expected to increase in the central and upper part of the Koshi Basin. Moreover, water yield is also expected to intensify in most parts of the basin (Bharati et al., 2014). Results further indicate that the flows in the West Seti River are expected to increase whereas the flows in the Budhi Ganga River are expected to decrease. The average streamflow in the basin is expected to increase by 5.9% in the NF and by 19.2% in the MF for RCP 4.5 and by 15% in the NF and by 11.8% in the MF un-

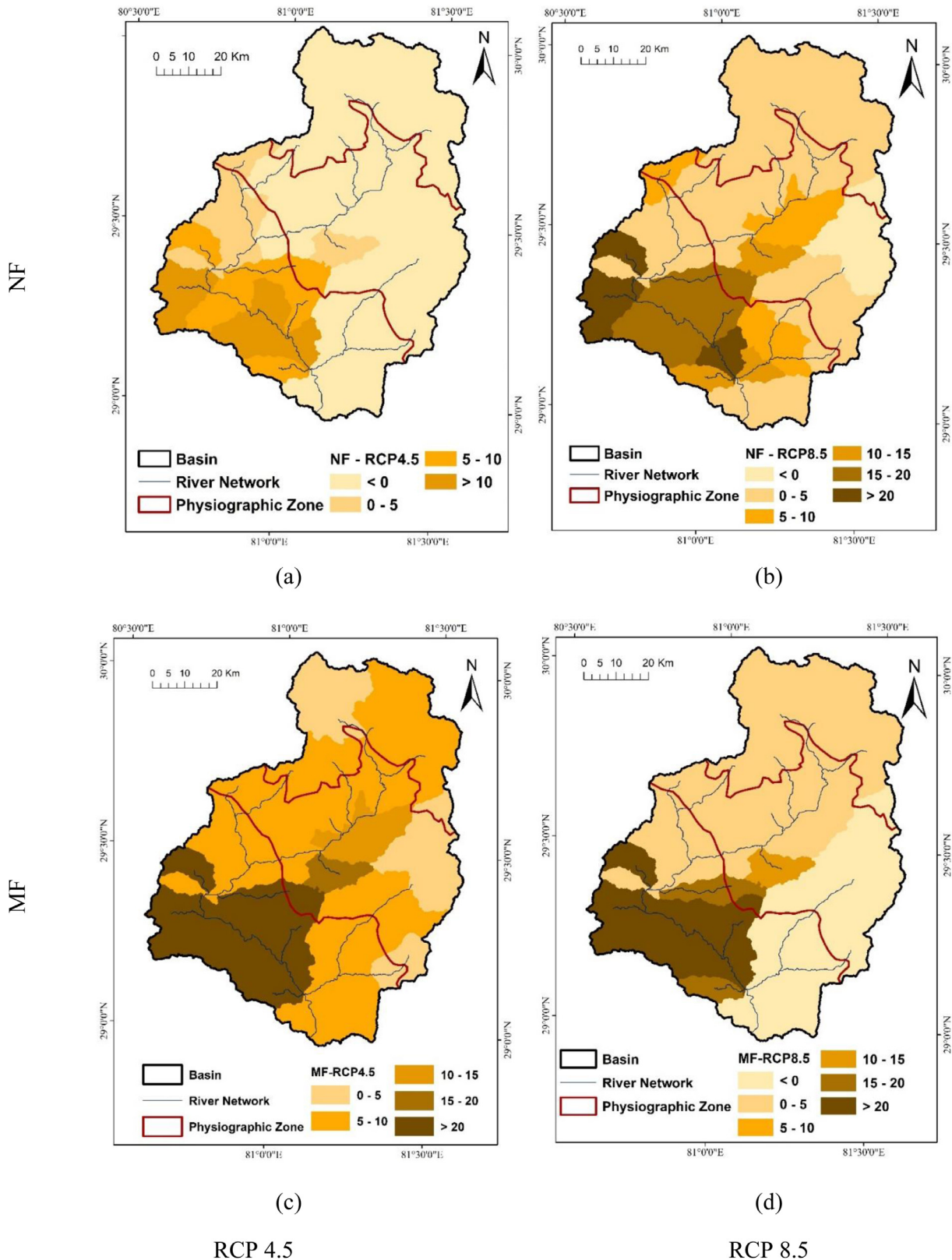


Fig. 7. Percentage changes in water yield under RCP 4.5 and RCP 8.5 scenarios in the NF (a) (b) (Upper Panel) and the MF (Lower Panel) (c) (d) in the WSRB.

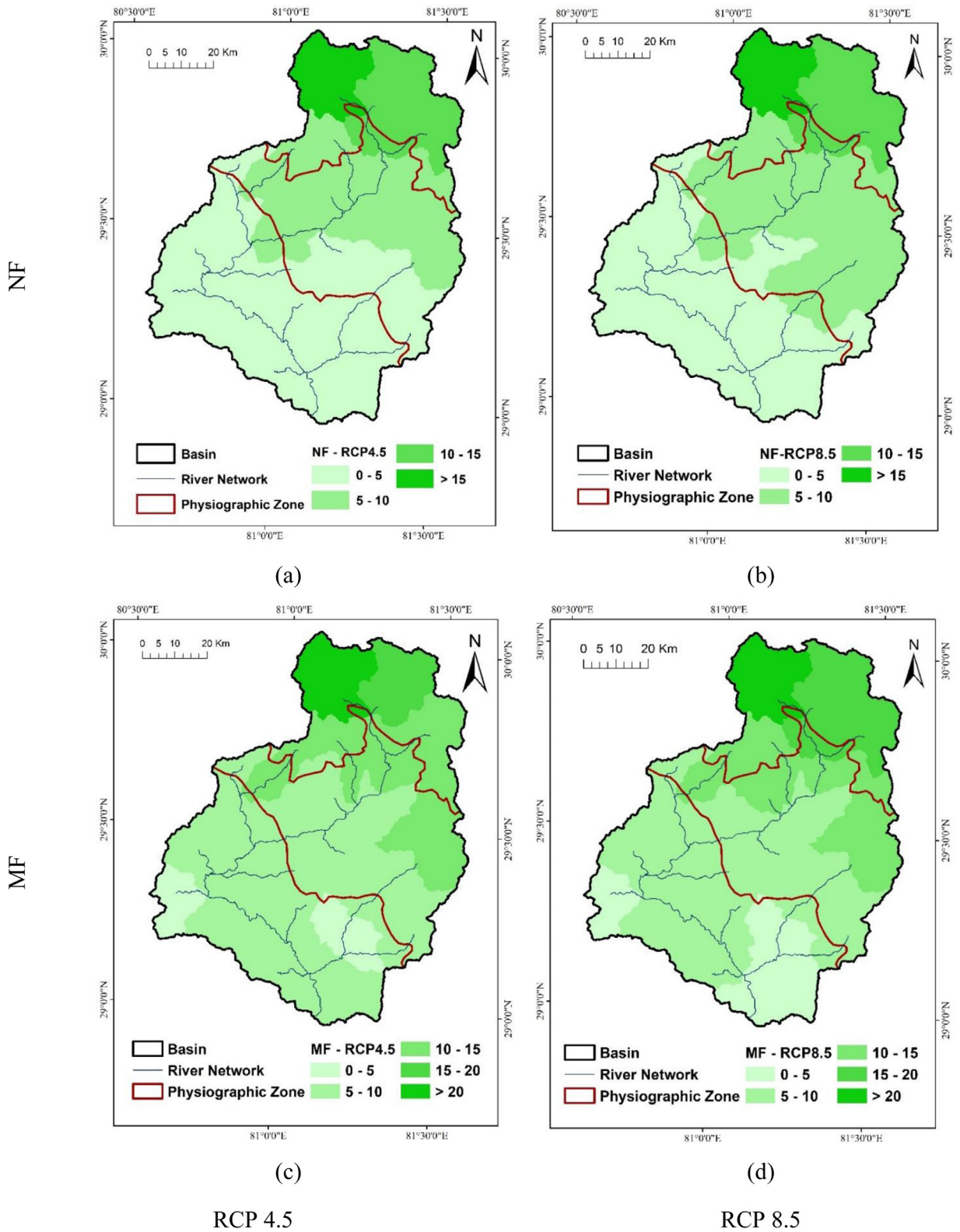


Fig. 8. Percentage change in evapotranspiration under RCP 4.5 and RCP 8.5 scenarios in the NF (a) (b) (Upper Panel) and the MF (Lower Panel) (c) (d) in the WSRB.

Table 5

Absolute and percentage changes in future flows, relative to the baseline period (1986 to 2005) at the Banga Stream Gauge under RCP 4.5 and RCP 8.5 in the WSRB.

	Base period streamflow (m ³ /s)	Future Period	RCP 4.5		RCP 8.5	
			(m ³ /s)	(% change)	(m ³ /s)	(% change)
Q5	971.82	NF	1048	7.9	1083	11.5
		MF	1103	13.5	1059	9.9
Q50	146.3	NF	154	5.9	168	15.0
		MF	174	19.2	163	11.8
Q95	34.36	NF	26	-23.8	27	-19.2
		MF	31	-7.9	27	-19.4

der RCP 8.5. Similar trends are reported in a study in the Purna river basin of India by Nilawar and Waikar (2019) as well as in the Blue Nile basin in Ethiopia with an increase of 22 to 27% in streamflow (Wagena et al., 2016). In addition, under different climate change scenarios, the change in river flow up to 36% is reported in the Yarmouk river which is a transboundary river basin between Jordan and Syria (Abdulla and Al-Shurafat, 2020) and between 7.6% to 13.5% increase in the Bang Pakong-Prachin Buri River Basin in Thailand (Okwala et al., 2020).

Table 5 presents the results for the high (Q5, flow equaled or exceeded at 5% of the time), average (Q50, flow equaled or exceeded at 50% of the time), and low (Q95, flow equaled or exceeded at 95% of the time) flows during the near future and mid future periods for RCP 4.5 and RCP 8.5. The low flows in the river are expected to decrease whereas the high flows are expected to increase in the future. A similar trend of high magnitude flood occurrence is expected in the Bang Pakong-Prachin-Buri River Basin in Thailand (Okwala et al., 2020) and eight major river basins of Eastern China (Xia et al., 2017). In addition, increase in dry months resulting in frequent drought occurrence is expected in the Pajaro River Basin in the U.S.A. (Bhandari et al., 2020) as well as dominance of dry spells till the end of the century is expected in Ankara in Turkey (Danandeh et al., 2020). This could result in less water availability in the dry season. In contrast, during the rainy season, the increased flows may result in flooding. This, however, gives an opportunity to harness the river flows during the rainy season by developing water resources which could help in mitigating the scarcity of water in the dry season. The natural balance of the basin water's balance components and its ecosystem services may be altered by changes in streamflow, which may have an adverse effect on the Himalayan catchments (Khadka et al., 2014). Analysis of the flow duration curve shows the impact of climate change on different flow regimes in the WSRB (Fig. 9).

The low flows also indicate less water in the basin during the dry season, which may result in drought and that would affect meeting the water demand as well. These variations in the frequency of high flow and scarcity of water will hinder the volume and quality of proper drinking water and agricultural activity as well as ecosystem planning (Singh and Goyal, 2017). Therefore, proper watershed and water management interventions like afforestation, on-farm conservation, infiltration ponds, reservoirs operation policies, water harvesting measures, and water

demand management should be promoted. In addition, provisions for proper drinking water, reservoir safety, and early warning systems should be considered as preventive measures in the flood prone areas to promote better water resources management in the basin (Nilawar and Waikar, 2019).

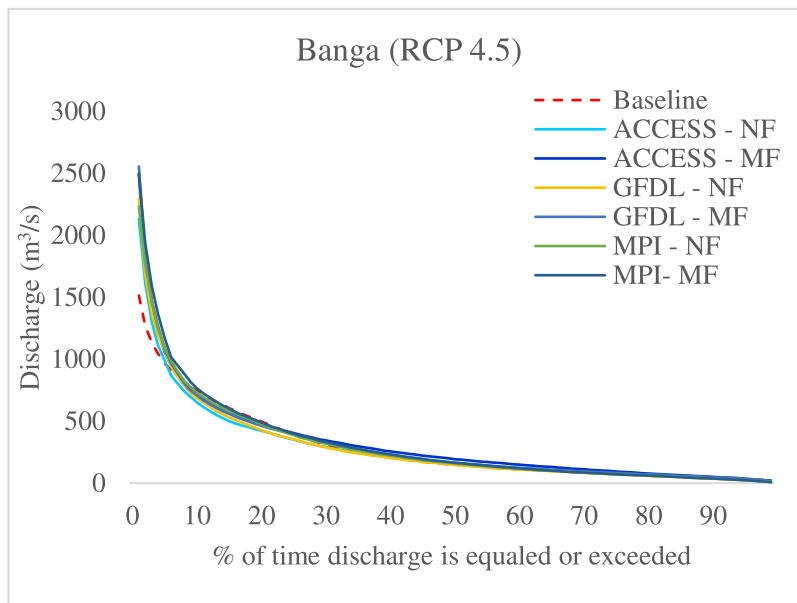
Land use changes must also be taken into consideration along with climate change in such hydrologic studies. Various studies have reported uncertainties in future climate and forecast of streamflow. Hagemann et al., (2013) identified hydrologic model uncertainty as predominant in impact assessment. Further studies are recommended on analyzing various uncertainties involved in such impact assessment and analysis.

Based on this study's results, it is recommended that the expected increase in river flows in the future should be considered as an opportunity by relevant ministries and departments/agencies in Nepal for better planning and management of water resources in the basin. Especially, considering the climate adapted West Seti Hydroelectric Project which lies in the High Mountain region, several aspects are to be considered for better watershed management to reduce disaster risk.

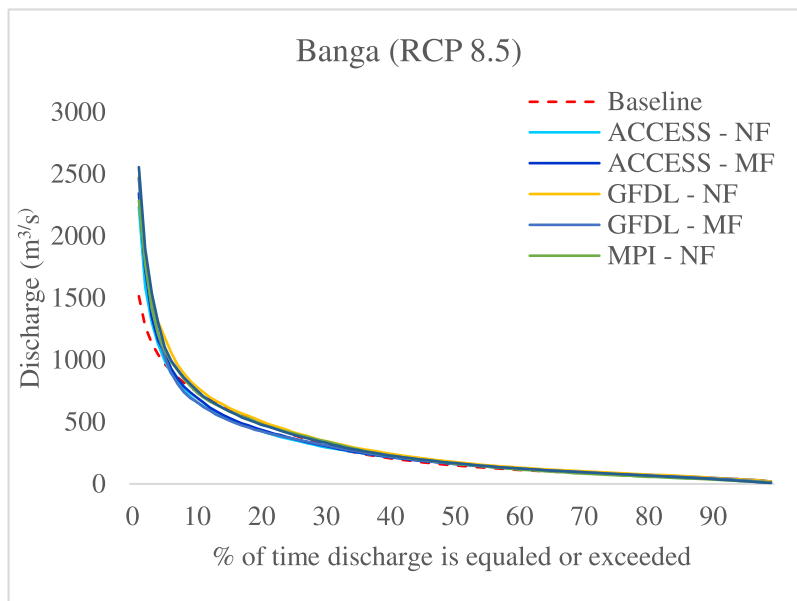
4. Conclusions

This research in the West Seti River Basin (WSRB) of Nepal evaluated the climate change impacts on water balance components and hydrological extremes. The SWAT model was used for the hydrological simulations in the basin. The performance of the model was robust in terms of simulating hydrological flow patterns for both daily and monthly time-series. Future climatic conditions were represented by three RCMs under RCP 4.5 and 8.5. Bias correction of RCMs projected temperatures and precipitation was done using quantile mapping and linear scaling methods respectively.

Both maximum and minimum temperatures in the future are projected to increase in the study basin. However, the minimum temperature will experience a higher increase compared to the maximum temperature. A higher fluctuation with an overall rise in precipitation is expected in the WSRB in future periods. Precipitation is expected to increase more in the mid future period for both RCP 4.5 and 8.5 compared to the near future. The Middle Mountain region will experience an increase in average annual precipitation under RCP 4.5 and 8.5, in both near future and mid future conditions compared to High Mountain and



(a)



(b)

Fig. 9. Flow duration curve at the outlet of WSRB under (a) RCP 4.5 and (b) RCP 8.5 scenarios.

High Himalayas. As expected, due to an increase in precipitation, water yield in all physiographic regions and under all future periods is likely to increase with a higher rise in the Middle Mountain region. It is interesting to note that the evapotranspiration in the High Himalayas is expected to have a higher increase than the Middle Mountain and High Mountain regions for both RCP scenarios and future periods. Likewise, most part of the basin will experience a rise in streamflow for both RCP 4.5 and 8.5 in comparison to the baseline. Reduction in the low flows and increase in

the high flows are expected in the study basin, which indicates that water resource development such as for irrigation and hydropower could be options to explore and avail the opportunity due to expected climate change in the basin. Whereas the proposed development project, West Seti Hydropower should consider the climate induced risk at the planning stage. Similarly, the development of other water related infrastructures should also consider climate-related risks considering climate variability and change in the area.

Declaration of Competing Interest

The authors declare that they have no known competing financial interests or personal relationships that could have appeared to influence the work reported in this paper.

Acknowledgements

The authors would like to thank Mr. Pabitra Gurung and Dr. Anshul Agarwal for providing data, allocating time, and assisting in developing the hydrological model. Furthermore, the authors express their sincere thanks and appreciation to project 'Excellence Centers for Exchange and Development - International Network on Sustainable Water Management in Developing Countries' (EXCEED – SWIN-DON) for providing support to the first author during student exchange program at Technical University of Braunschweig (TUBS), Germany.

Supplementary materials

Supplementary material associated with this article can be found, in the online version, at doi:[10.1016/j.ecohyd.2020.07.001](https://doi.org/10.1016/j.ecohyd.2020.07.001).

References

- Abdulla, F., Al-Shurafat, A.W., 2020. Assessment of the Impact of Potential Climate Change on the Surface Water of a Trans-boundary Basin: Case Study Yarmouk River. *Procedia Manufacturing* 44, 172–179. doi:[10.1016/j.promfg.2020.02.219](https://doi.org/10.1016/j.promfg.2020.02.219).
- Anjum, M.N., Ding, Y., Shangguan, D., 2019. Simulation of the projected climate change impacts on the river flow regimes under CMIP5 RCP scenarios in the westerlies dominated belt, northern Pakistan. *Atmospheric Research* 227, 233–248. doi:[10.1016/j.atmosres.2019.05.017](https://doi.org/10.1016/j.atmosres.2019.05.017).
- Aryal, R.S., Rajkarnikar, G., 2011. Water Resources of Nepal in the Context of Climate Change. Water and Energy Commission Secretariat (WECS), Nepal <https://www.weecs.gov.np/uploaded/water-reource-climate-change.pdf>.
- Ayivi, F., Jha, M.K., 2018. Estimation of water balance and water yield in the Reedy Fork-Buffalo Creek Watershed in North Carolina using SWAT. *International Soil and Water Conservation Research* 6 (3), 203–213. doi:[10.1016/j.iswcr.2018.03.007](https://doi.org/10.1016/j.iswcr.2018.03.007).
- Babel, M.S., Bhusal, S.P., Wahid, S.M., Agarwal, A., 2014. Climate change and water resources in the Bagmati River Basin, Nepal. *Theoretical and applied climatology* 115 (3–4), 639–654. doi:[10.1007/s00704-013-0910-4](https://doi.org/10.1007/s00704-013-0910-4).
- Bajracharya, A.R., Bajracharya, S.R., Shrestha, A.B., Maharjan, S.B., 2018. Climate change impact assessment on the hydrological regime of the Kaligandaki Basin, Nepal. *Science of the Total Environment* 625, 837–848. doi:[10.1016/j.scitotenv.2017.12.332](https://doi.org/10.1016/j.scitotenv.2017.12.332).
- Bartlett, R., Bharati, L., Pant, D., Hosterman, H., McCornick, P.G., 2010. Climate change impacts and adaptation in Nepal, 139. *IWMI*. <http://www.environmentportal.in/files/Climate%20Change%20Impacts.pdf>.
- Bhandari, R., Kalra, A., Kumar, S., 2020. Analyzing the effect of CMIP5 climate projections on streamflow within the Pajaro River Basin. *Open Water Journal* 6 (1), 5. https://scholarsarchive.byu.edu/cgi/viewcontent.cgi?article=1100&context=openwater&fbclid=IwAR3cMauH-AZjT1a2VpckEBL96q1_4NI0GGH5xNmW7B9lv7Nm-Vuex67u0.
- Bharati, L., Gurung, P., Jayakody, P., Smakhtin, V., Bhattarai, U., 2014. The projected impact of climate change on water availability and development in the Koshi Basin, Nepal. *Mountain Research and Development* 34 (2), 118–131. doi:[10.1659/MRD-JOURNAL-D-13-00096.1](https://doi.org/10.1659/MRD-JOURNAL-D-13-00096.1).
- Danandeh Mehr, A., Sorman, A.U., Kahya, E., Hesami Afshar, M., 2020. Climate change impacts on meteorological drought using SPI and SPEI: case study of Ankara, Turkey. *Hydrological Sciences Journal* 65 (2), 254–268. doi:[10.1080/02626667.2019.1691218](https://doi.org/10.1080/02626667.2019.1691218).
- Buishand, T.A., 1982. Some methods for testing the homogeneity of rainfall records. *Journal of Hydrology* (58) 11–27. doi:[10.1016/0022-1694\(82\)90066-X](https://doi.org/10.1016/0022-1694(82)90066-X).
- Fang, G., Yang, J., Chen, Y., Zammit, C., 2015. Comparing bias correction methods in downscaling meteorological variables for a hydrologic impact study in an arid area in China. *Hydrology and Earth System Sciences* 19 (6), 2547–2559. doi:[10.5194/hess-19-2547-2015](https://doi.org/10.5194/hess-19-2547-2015).
- Ficklin, D.L., Luo, Y., Luedeling, E., Zhang, M., 2009. Climate change sensitivity assessment of a highly agricultural watershed using SWAT. *Journal of Hydrology* 374 (1–2), 16–29. doi:[10.1016/j.jhydrol.2009.05.016](https://doi.org/10.1016/j.jhydrol.2009.05.016).
- Fontaine, T., Cruickshank, T., Arnold, J., Hotchkiss, R., 2002. Development of a snowfall–snowmelt routine for mountainous terrain for the soil water assessment tool (SWAT). *Journal of hydrology* 262 (1–4), 209–223. doi:[10.3394/0380-1330\(2006\)32\[471:AOSYFA\]2.0.CO;2](https://doi.org/10.3394/0380-1330(2006)32[471:AOSYFA]2.0.CO;2).
- Gosling, S.N., Arnell, N.W., 2016. A global assessment of the impact of climate change on water scarcity. *Climatic Change* 134 (3), 371–385. doi:[10.1007/s10584-013-0853-x](https://doi.org/10.1007/s10584-013-0853-x).
- Grusson, Y., Sun, X., Gascoin, S., Sauvage, S., Raghavan, S., Anctil, F., Sáchez-Pérez, J.-M., 2015. Assessing the capability of the SWAT model to simulate snow, snow melt and streamflow dynamics over an alpine watershed. *Journal of Hydrology* 531, 574–588. doi:[10.1016/j.jhydrol.2015.10.070](https://doi.org/10.1016/j.jhydrol.2015.10.070).
- Gurung, P., Bharati, L., Karki, S., 2015. Impact of climate change and watershed interventions on water balance and crop yield in West Seti river sub-basin of Nepal. *Journal of Hill Agriculture* 6 (2), 219–227. doi:[10.5958/2230-7338.2015.00051.8](https://doi.org/10.5958/2230-7338.2015.00051.8).
- Hagemann, S., Chen, C., Clark, D.B., Folwell, S., Gosling, S.N., Haddeland, I., Hanasaki, N., Heinke, J., Ludwig, F., Voss, F., 2013. Climate change impact on available water resources obtained using multiple global climate and hydrology models. *Earth System Dynamics* 4 (1), 129–144. doi:[10.5194/esd-4-129-2013](https://doi.org/10.5194/esd-4-129-2013).
- Immerzeel, W., Pellicciotti, F., Bierkens, M., 2013. Rising river flows throughout the twenty-first century in two Himalayan glacierized watersheds. *Nature geoscience* 6 (9), 742. doi:[10.1038/ngeo1896](https://doi.org/10.1038/ngeo1896).
- IPCC, 2014. Climate change 2014: impacts, adaptation, and vulnerability. IPCC Working Group II https://www.ipcc.ch/site/assets/uploads/2018/02/WGIIAR5-PartA_FINAL.pdf.
- Khadka, D., Babel, M.S., Shrestha, S., Tripathi, N.K., 2014. Climate change impact on glacier and snow melt and runoff in Tamakoshi basin in the Hindu Kush Himalayan (HKH) region. *Journal of Hydrology* 511, 49–60. doi:[10.1016/j.jhydrol.2014.01.005](https://doi.org/10.1016/j.jhydrol.2014.01.005).
- Lutz, A., Immerzeel, W., Shrestha, A., Bierkens, M., 2014. Consistent increase in High Asia's runoff due to increasing glacier melt and precipitation. *Nature Climate Change* 4 (7), 587. doi:[10.1038/nclimate2237](https://doi.org/10.1038/nclimate2237).
- Maraun, D., 2013. Bias correction, quantile mapping, and downscaling: Revisiting the inflation issue. *Journal of Climate* 26 (6), 2137–2143. doi:[10.1175/JCLI-D-12-00821.1](https://doi.org/10.1175/JCLI-D-12-00821.1).
- Matthews, E., 2001. Understanding the FRA 2000. Forest briefing no. 1, 12. World Resources Institute, Washington, DC <https://pdfs.semanticscholar.org/1988/0fa1ef5c92e6008ca2913c2b5ff795bb0342.pdf>.
- Middelkoop, H., Daamen, K., Gellens, D., Grabs, W., Kwadijk, J.C., Lang, H., Parmet, B.W., Schädlér, B., Schulla, J., Wilke, K., 2001. Impact of climate change on hydrological regimes and water resources management in the Rhine basin. *Climatic change* 49 (1–2), 105–128. doi:[10.1023/A:1010784727448](https://doi.org/10.1023/A:1010784727448).
- Mishra, Y., Nakamura, T., Babel, M.S., Ninsawat, S., Ochi, S., 2018. Impact of climate change on water resources of the Bheri River Basin, Nepal. *Water* 10 (2), 220. doi:[10.3390/w10020220](https://doi.org/10.3390/w10020220).
- Moriasi, D.N., Arnold, J.G., Van Liew, M.W., Bingner, R.L., Harmel, R.D., Veith, T.L., 2007. Model evaluation guidelines for systematic quantification of accuracy in watershed simulations. *Transactions of the ASABE* 50 (3), 885–900. <https://swat.tamu.edu/media/90109/moriasimodeleval.pdf>.
- Neitsch, S.L., Arnold, J.G., Kiniry, J.R., Williams, J.R., 2011. Soil and water assessment tool theoretical documentation version 2009. Texas Water Resources Institute <https://swat.tamu.edu/media/99192/swat2009-theory.pdf>.
- Nilawar, A.P., Waikar, M.L., 2019. Impacts of climate change on streamflow and sediment concentration under RCP 4.5 and 8.5: A case study in Purna river basin, India. *Science of The Total Environment* 650, 2685–2696. doi:[10.1016/j.scitotenv.2018.09.334](https://doi.org/10.1016/j.scitotenv.2018.09.334).
- Okwala, T., Shrestha, S., Ghimire, S., Mohanasundaram, S., Datta, A., 2020. Assessment of climate change impacts on water balance and hydrological extremes in Bang Pakong-Prachin Buri river basin, Thailand. *Environmental Research*, 109544. doi:[10.1016/j.envres.2020.109544](https://doi.org/10.1016/j.envres.2020.109544).
- Pandey, V.P., Dhaubanjari, S., Bharati, L., Thapa, B.R., 2019. Hydrological response of Chamelia watershed in Mahakali Basin to climate change. *Science of the Total Environment* 650, 365–383. doi:[10.1016/j.scitotenv.2018.09.053](https://doi.org/10.1016/j.scitotenv.2018.09.053).
- Shrestha, A.B., Aryal, R., 2011. Climate change in Nepal and its impact on Himalayan glaciers. *Regional Environmental Change* 11 (1), 65–77. doi:[10.1007/s10113-010-0174-9](https://doi.org/10.1007/s10113-010-0174-9).

- Siddiqui, S., Bharati, L., Pant, M., Gurung, P. and Rakkhal, B., 2012. Nepal: building climate resilience of watersheds in mountain eco-regions climate change and vulnerability mapping in watersheds in middle and high mountains of Nepal. <https://hdl.handle.net/10568/34713>
- Singh, V., Goyal, M.K., 2017. Curve number modifications and parameterization sensitivity analysis for reducing model uncertainty in simulated and projected streamflows in a Himalayan catchment. *Ecological engineering* 108, 17–29. doi:10.1016/j.ecoleng.2017.08.002.
- Smith, J.B., Hulme, M., Jaagus, J., Keevallik, S., Mekonnen, A., Hailemariam, K., 1998. Climate change scenarios. UNEP Handbook on Methods for Climate Change Impact Assessment and Adaptation Studies, 2 3-1 http://www.ivm.vu.nl/en/Images/UNEPHandbookEBA2ED27-994E-4538-B0F0C424C6F619FE_tcm234-102683.pdf.
- Stocker, T., 2014. Climate change 2013: the physical science basis: Working Group I contribution to the Fifth assessment report of the Intergovernmental Panel on Climate Change. Cambridge University Press https://www.ipcc.ch/site/assets/uploads/2018/02/WG1AR5_all_final.pdf.
- Tapiador, F.J., Moreno, R., Navarro, A., Sánchez, J.L., García-Ortega, E., 2019. Climate classifications from regional and global climate models: Performances for present climate estimates and expected changes in the future at high spatial resolution. *Atmospheric research* 228, 107–121. doi:10.1016/j.atmosres.2019.05.022.
- Taylor, K.E., Stouffer, R.J., Meehl, G.A., 2012. An overview of CMIP5 and the experimental design. *Bulletin of the American Meteorological Society* 93, 485–498. doi:10.1016/j.scitotenv.2019.134163.
- Wagena, M.B., Sommerlot, A., Abiy, A.Z., Collick, A.S., Langan, S., Fuka, D.R., Easton, Z.M., 2016. Climate change in the Blue Nile Basin Ethiopia: implications for water resources and sediment transport. *Climatic change* 139 (2), 229–243. doi:10.1007/s10584-016-1785-z.
- Xia, J., Duan, Q.Y., Luo, Y., Xie, Z.H., Liu, Z.Y., Mo, X.G., 2017. Climate change and water resources: Case study of Eastern Monsoon Region of China. *Advances in Climate Change Research* 8 (2), 63–67. doi:10.1016/j.accre.2017.03.007.
- Yatagai, A., Kamiguchi, K., Arakawa, O., Hamada, A., Yasutomi, N., Kitoh, A., 2012. APHRODITE: Constructing a long-term daily gridded precipitation dataset for Asia based on a dense network of rain gauges. *Bulletin of the American Meteorological Society* 93 (9), 1401–1415. doi:10.1175/BAMS-D-11-00122.1.